Vanadyl complexes with dansyl-labelled di-picolinic acid ligands: synthesis, phosphatase inhibition activity and cellular uptake studies

Juliet Collins,[1,2] Agostino Cilibrizzi,[1,2] Marina Fedorova,[1] Gillian Whyte,[1] Lok Hang Mak[1], Inna Guterman[1], Robin Leatherbarrow,[1,2,3] Rudiger Woscholski,[1,2] Ramon Vilar[1,2]*

[1]*Department of Chemistry, Imperial College London, London SW7 2AZ, UK*

[2]*Institute of Chemical Biology, Imperial College London, London SW7 2AZ, UK*

[3] *Current address: Liverpool John Moores University, Egerton Court, Liverpool L1 2UA, UK*

*Corresponding author: r.vilar@imperial.ac.uk

Abstract

Vanadium complexes have been previously utilised as potent inhibitors of cysteine based phosphatases (CBPs). Herein, we present the synthesis and characterisation of two new fluorescently labelled vanadyl complexes (**14** and **15**) with bridged di-picolinic acid ligand. These compounds differ significantly from previous vanadyl complexes with phosphatase inhibition properties in that the metal-chelating part is a single tetradentate unit, which should afford greater stability and scope for synthetic elaboration then the earlier complexes. These new complexes inhibit a selection of cysteine based phosphatases (CBPs) in the nM range with some selectivity. Fluorescence spectroscopic studies (including fluorescence anisotropy) were carried out to demonstrate that the complexes are not simply acting as vanadyl delivery vehicles but they interact with the proteins. Finally, we present preliminary fluorescence microscopy studies to demonstrate that the complexes are cell permeable and localise throughout the cytoplasm of NIH3T3 cells.

Introduction

Cysteine based phosphatases (CBPs) are a large family of enzymes that are defined by a cysteine containing motif (CX_5R) in their active site and include the protein tyrosine phosphatases (PTPs) and inositol lipid phosphatases[1]. While the former counteract the action of tyrosine protein kinases the latter balance inositol lipid kinases.[2,3] Both play an important role in the regulation of phosphorylation in cells, which in turn impacts cellular signalling and function.[3,4] Mutation or dysfunction of many members of this family of enzymes have been implicated in a range of diseases including immune and neurodegenerative disorders, cancer, diabetes and obesity, as well as having a role in inflammatory responses.[5,6] Given the importance of CBPs in disease progression, they are regarded as interesting targets for drug development, with a variety of inhibitors being reported.[5,7-14] One subset of these inhibitors are metal ions and their complexes including vanadium, zinc, copper and others, which have shown potent inhibition of PTPs *in vitro* and *in vivo*.[11,15-19] In particular, a variety of complexes with both vanadium(IV) and vanadium(V) centres have been developed and characterised for their CBP inhibition properties[7,10,20-27] including several examples with picolinic acid and its derivatives as ligands.[28-33] The potency of these inhibitors against PTPs and lipid phosphatases can be tuned as a function of the ligand, the vanadium coordination number and the oxidation state. For example, the vanadyl complexes $V^{IV}O$(picolinic acid)$_2$ and $V^{IV}O$(3-hydroxypicolinic acid)$_2$ (**1** and **2**, Fig.1) have been shown to inhibit specific phosphatases at nanomolar concentrations.[29,31]

Using as a starting point vanadyl-picolinate complexes such as **1** and **2**, we were interested in developing novel inhibitors for PTPs and lipid phosphatases with improved features. We hypothesised that more robust vanadyl complexes could be obtained by using ligands where the two picolinic acids were covalently linked by an appropriate spacer to yield a tetradentate ligand (Fig. 2). Furthermore, the linker would offer the potential for further

chemical functionalisation, such as allowing addition of a fluorophore to track cellular uptake and localisation of the resulting vanadyl complexes. Thus, herein we report on the synthesis and characterisation of two new fluorescently labelled di-picolinic acid ligands (**8** and **13**, Fig. 2) and the corresponding vanadyl complexes (**14** and **15**, Fig. 3). We demonstrate that addition of the complexes to PTPs and lipid phosphatase leads to inhibition (in the nM range) of the enzymes' activity. We also show by fluorescence microscopy that the complexes are cell permeable.

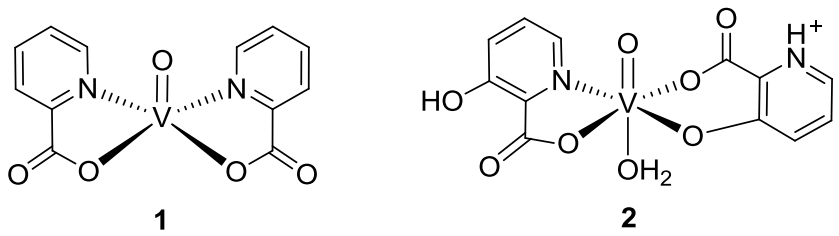

Fig. 1 Known vanadyl complexes with PTP and lipid phosphatase inhibitory properties.

Results and Discussion

Synthesis of ligands

The two new tetradentate ligands (**8** and **13**) were synthesised as shown in Fig. 2. 5-hydroxypicolinic acid methyl ester (**3**)[34] was reacted with the corresponding Boc-protected di-alcohol (**4** or **9**) via a Mitsunobu reaction using diethyl azodicarboxylate and triphenylphosphine. In both cases, after initial purification by column chromatography, the products (**5** and **10**) were obtained as a mixture with triphenylphosphine oxide. Optimisation of chromatographic conditions reduced the amount of triphenylphosphine oxide but it could

not be removed completely. The crude materials were used in the de-protection step which, after purification, yielded the corresponding amines **6** and **11** as pure compounds (as confirmed by ^{1}H NMR spectroscopy and mass spectrometry). The dansyl fluorophore was introduced *via* sulfonylation under anhydrous conditions in the presence of triethylamine to obtain **7** and **12**, which were taken forward to the final step for removal of the methyl protecting groups to give the corresponding ligands **8** and **13**. The formation of the desired products was confirmed by ^{1}H NMR spectroscopy (Fig. S1 and S2, Supporting Information) through the disappearance of the methyl peaks (at *ca*. 3.9 ppm); mass spectrometry provided further evidence for the formation of both **8** and **13**. Fluorescence emission spectroscopy confirmed the presence of the dansyl fluorophore in both the diethanolamine (**8**, Fig. S3 Supporting Information) and dipropanolamine (**13**) linked ligands with emission maxima at 538 nm and 528 nm respectively.

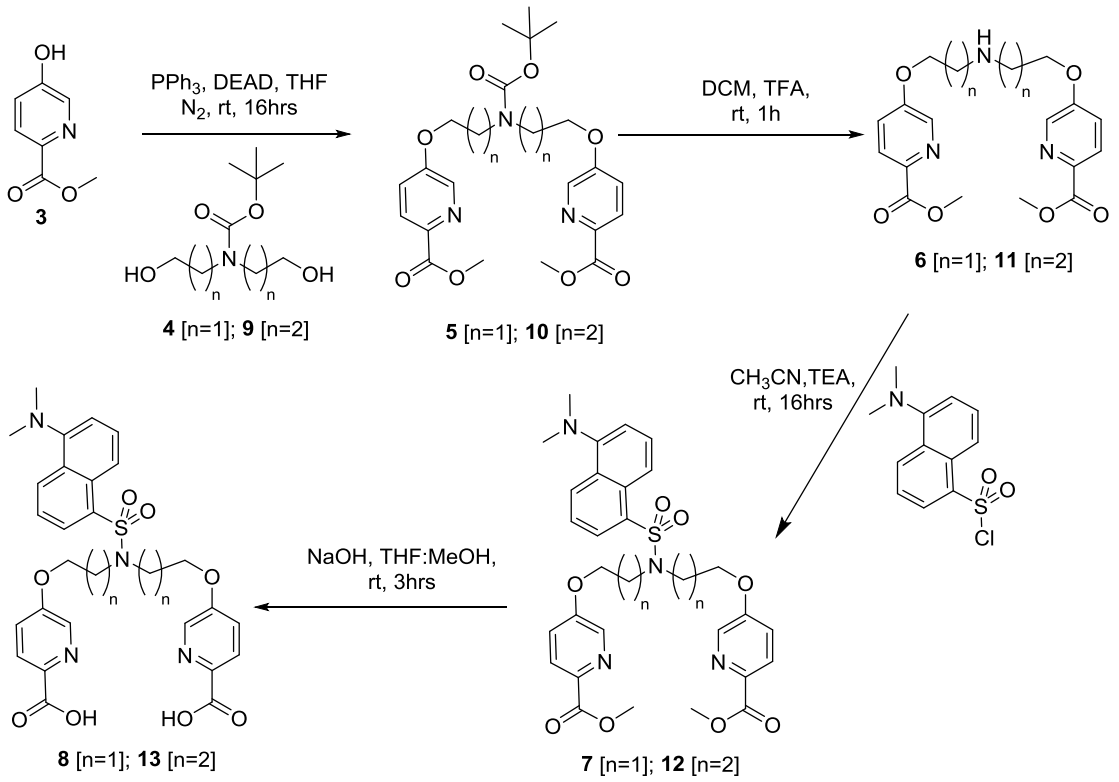

Fig. 2 Synthesis of fluorescently labelled ligands **8** and **13**.

Synthesis of vanadyl complexes

In order to prepare the vanadyl complexes, the corresponding ligand was dissolved in water (in the presence of $NaHCO_3$) and an aqueous solution of vanadyl sulphate slowly added. A clear change from a yellow solution to a dark green suspension was observed upon addition of $VOSO_4$ to the ligand. The new vanadyl complexes **14** and **15** were obtained as dark green solids and were characterised by spectroscopic and analytical techniques. MALDI-TOF mass spectrometry showed peaks corresponding to $[M+Na]^+$ in each case. The IR spectra of the two complexes shows peaks for the ligand at 1645-1572 cm^{-1} (which can be assigned to C=O, C=C and C=N) as well as a strong peak at 965 cm^{-1} and 961 cm^{-1} (assigned to V=O) for **14** and **15** respectively (Table 1). The formulation and purity of the complexes was confirmed by elemental analyses. Both vanadyl complexes are fluorescent (Table 1) although their emission intensities are lower than those of the corresponding free ligands.

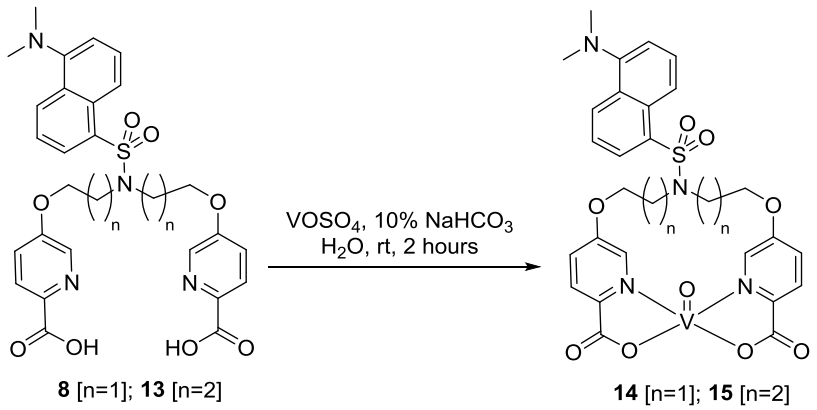

Fig. 3 Synthesis of vanadyl complexes **14** and **15** from the corresponding ligands (**8** and **13**) and vanadyl sulphate.

Table 1. Spectroscopic data for vanadyl complexes. The IR data was recorded using a solid sample of the corresponding compound while UV/Vis and emission spectroscopic data was collected using solutions in methanol (**14** and **15** at 30 μM**, 1** at 15 μM and **2** at 45 μM). Fluorescence data was recorded in Tris buffer (30 μM).

Compound	IR (V=O)/cm^{-1}	UV-vis λ_{max} /nm (ε/ M^{-1} cm^{-1})	Fluorescence λ_{max}(em)/nm
14	965	263 (4.86×10^4)	568
15	961	262 (7.37×10^4)	566
1	962	266 (7.78×10^3)	-
2	954	305 (9.8×10^3)	-

Phosphatase inhibition assays

In order to characterise the inhibitory potency of **14** and **15**, phosphatase inhibition assays against a selection of PTPs (PTP1B, LMW-PTP, VHR and SHP-2 – see Table 2 for abbreviations) as well as the inositol lipid phosphatase PTEN were carried out employing 3-*O*-methylfluorescein phosphate (OMFP) as a substrate.[28] As shown in Table 2 compounds **14** and **15** inhibit all PTPs tested in the mid to high nanomolar range, which is consistent with the inhibitory potency previously reported for compound **1** (Fig 1).[29,31] The IC_{50} value for **14** against LMW-PTP and PTEN is significantly higher than for the other enzymes while complex **15** has a significantly lower IC_{50} value for PTP1B than for any other of the tested phosphatases. These observations suggest that the complexes show some selectivity towards certain PTPs compared to others. There also seems to be an effect on the inhibitory properties of the complex on increasing the length of the linker from diethanolamine (**14**) to dipropanolamine (**15**) for VHR, SHP2, and LMW-PTP. The IC_{50} values for VHR and SHP2

are around two to three fold higher for compound **15** than **14** whereas the IC_{50} is reduced against LMW-PTP on increasing linker length. This suggests that varying the linker length could be used as a method to tune selectivity of the complex as the effect differs across the CBPs. As a control, we also carried out the inhibition studies with the free ligands (**8** and **13**) using VHR and LMW-PTP as representative examples of the phosphatases. No inhibition was observed up to a 1 μM concentration of the ligand and only minor effects were observed at 10 μM (Fig. S6 and S7, Supporting Information); this indicates that the free ligand does not contribute to the IC_{50} values reported in Table 2. We also carried out the inhibition studies using $VOSO_4$ as a control. As can be seen in Table 2, the inhibitor profile for $VOSO_4$ did not match with the one observed for compounds **14** and **15.** For example, $VOSO_4$ is more potent against SHP2, but significantly less potent for PTP1B, which is not what one would expect if the complexes are a delivery mechanism for vanadyl itself. Thus, the data suggests that **14** and **15** are not acting simply as a vanadyl delivery vehicle. This notion was explored in more depth using spectroscopy means (see next section).

Table 2 IC_{50} values (nM) of vanadyl complexes **14** and **15** (the data shown is ±standard deviation of triplicate repeats)

Compound	PTEN	PTP1B	VHR	SHP2	LMW-PTP
14	211±33	94±43	72±10	77±27	177±7
15	222±49	84±23	130±14	162±20	120±12
$VOSO_4$	-	151±16	120±60	71±80	117±40

PTEN = Phosphatase and tensin homolog. PTP1B = Protein-tyrosine phosphatase 1. SHP-2 = Src homology region 2 domain-containing phosphatase-2. LMW-PTP = Low molecular weight protein tyrosine phosphatase. VHR = dual specificity protein phosphatase 3. For assay conditions see experimental section.

Effects of enzyme on the fluorescence of vanadyl complexes

Having shown that the potency of **14, 15** and $VOSO_4$ for the selected PTPs is close to each other, it was of interest to corroborate the conclusion drawn from the data presented in table 2. In order to investigate the integrity of the complexes in the enzyme assays, we made use of the dansyl moiety within the ligand in a number of fluorescence spectroscopic studies. Upon coordination of vanadyl to ligands **8** and **13**, the emission of the dansyl decreases, which can be employed to monitor the integrity of the complexes while interacting with the enzymes. Therefore, we first studied whether the fluorescence of the ligand in complex **14** could be recovered by removing the vanadyl from the corresponding complex with EDTA, a strong vanadyl chelator.[23] As can be seen in Figure 4, addition of an excess of EDTA (1 mM) to complex **14** (30 μM), restored the fluorescence of the ligand in the absence of enzyme. Having established that EDTA can indeed remove vanadyl from the complexes and in doing so change the fluorescence of the ligand, we investigated the effect of LMW-PTP (as a representative example of the PTPs) on the emission of complex **14**. As can been seen in Figure 4, incubation of **14** with LMW-PTP did not restore the emission of the ligand which suggests that the vanadyl is still coordinated to ligand **8** in the presence of the enzyme. A control experiment was carried out in which the compound was incubated with both EDTA and the enzyme and the emission intensity compared to that of the corresponding ligand under the same conditions. Interestingly, in this case full restoration of the emission was not observed after 5 minutes incubation (see Fig. S4, Supplementary Information) in spite of the presence of EDTA. Complete restoration was, however, observed after 2 hours incubation (see Fig. 4). These experiments were also carried out with ligand **13** and complex **15** and the same pattern of results was observed (see Fig S5, Supplementary Information, i.e. 2 hours incubation).

Taken together these observations imply that the enzyme LMW-PTP binds to the intact complex (as defined by the vanadyl being near the fluorophore-ligand) and in doing so 'protects' the tightly bound complexes from EDTA. However, we cannot rule out the possibility that the vanadyl, while still bound to the ligand, may form new interactions with the enzymes, which would imply that the vanadyl would exchange partially coordination sites between ligand and enzyme. We should also note that the interaction between the vanadium complexes and the Tris buffer used in these studies is unlikely to affect the observations. Previous studies have shown that such interactions are weak (i.e. high mM).[35] Furthermore, as we have demonstrated in this study, EDTA is required to remove the vanadium centre from the complex (in Tris buffer). Consequently, under the conditions of our studies, Tris is an appropriate buffer.

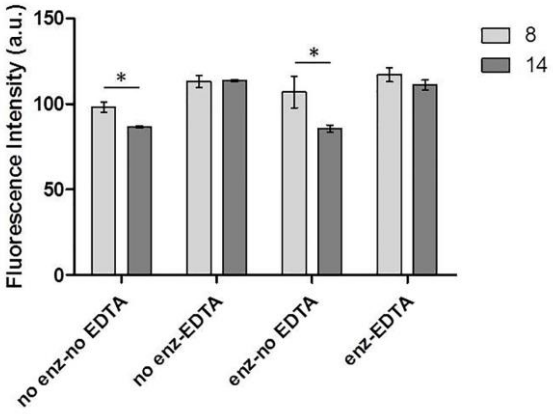

Fig.4 Fluorescence intensity at 560 nm of a 30 μM solution of ligand **8** and complex **14** in the presence or absence of LMW-PTP (Enz) and 1 mM EDTA in Tris buffer containing 1 mM DTT. Reading was taken after 2 hours incubation at room temperature. Intensity is recorded ±standard deviation of triplicate repeats. A statistical analysis has been performed showing that the difference between the fluorescence intensity of **8** and **14** incubated with enzyme in the absence of EDTA (1st and 3rd bar pairs in this figure) are statistically significant (*$p < 0.05$).

To investigate this further, we carried out fluorescence anisotropy studies of complex **14** in the presence and absence of LMW-PTP (as model enzyme). This type of studies is widely used to investigate the interaction between an emissive molecule and large bio-

molecules (such as proteins). This technique relies on the change in rotational correlation time of the fluorophore (in this case our dansyl-labelled vanadyl complex) upon interaction with a large molecule (in this case LMW-PTP). As can be seen in Fig. 5(a), addition of the enzyme to the complex led to an increase in the fluorescence anisotropy (reaching a maximum at *ca*. 2 equivalents of the enzyme) consistent with an interaction of the complex with the enzyme.

We then investigated the effect that EDTA has on the fluorescence anisotropy of complex **14** pre-bound to LMW-PTP. As Fig. 5(b) shows, the fluorescence anisotropy was reduced within an hour to the level of the enzyme-free sample suggesting that when the vanadyl is sequestered by the EDTA the fluorescent ligand no longer associates with the enzyme. Control studies with the free ligand were also carried out. The fluorescence anisotropy of **8** under the same experimental conditions (see caption in Fig. 5) was 0.20 and in the presence of enzyme (36 μM) was 0.21. This clearly demonstrates that the free ligand does not interact with the enzyme and therefore the changes observed with complex **14** are due to binding of the complex with the protein.

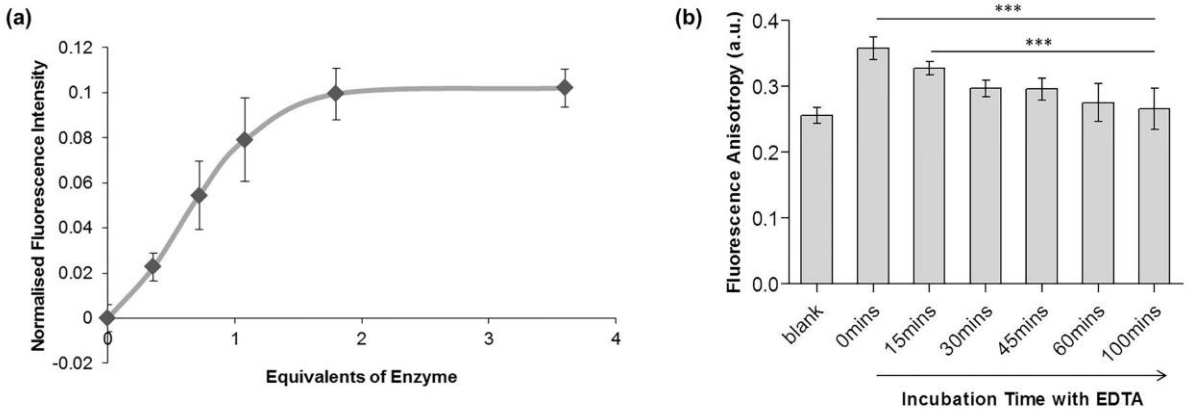

Fig.5 (a) Fluorescence anisotropy of **14** (10 μM) in the presence of increasing concentrations of LMW-PTP (0-36 μM). (b) Fluorescence anisotropy of **14** (10 μM) in the absence or presence of LMW-PTP and over 100 minutes of incubation with the enzyme and 1 mM EDTA. Readings were taken in 100mM Tris buffer solution with 1mM DTT in a 200μL fluorescence cuvette. Excitation wavelength is 340 nm, emission recorded at 560 nm. The error is shown as the standard deviation of 6 readings from two independent experiments. Significant differences (5% cut-off for significance) to the

"buffer + compound" data are indicated by stars (* $p < 0.05$; ** $p < 0.01$; *** $p < 0.001$). The blank control used 50% glycerol in elution buffer to mimic the enzyme solution as the viscosity of the mixture would have an effect on the polarisation.

The spectrofluorimetric data shown in Figures 4 and 5 clearly indicate that the complex does not break completely apart in the presence of the enzyme under physiological conditions. There have been extensive studies in the literature aimed at understanding the mode of action of vanadium complexes in the context of their CBP inhibition properties. There is considerable evidence suggesting that such complexes act as prodrugs releasing the active vanadium species in biological media.[36] Interestingly our data suggests that, under the conditions used, the vanadium complexes do not break apart completely.

Cellular uptake studies

In order for the complexes **14** and **15** to be utilised as PTPs inhibitors in a cellular environment their ability to be taken up into cells would have to be confirmed. Compound **14** was chosen as a representative complex and thus, NIH3T3 cells were incubated with three different concentrations of **14** (1, 5 and 10 μM) for 24 hours at 37 ºC. The cells were subsequently analysed by fluorescence microscopy. As can be seen in Fig. 6, the complex (green) is widely taken up by cells. Under these conditions, the complex is localised throughout the cell, but seems to be enriched in some structures within the nucleus and the perinuclear region. This is in agreement with the known subcellular localisation of PTEN and VHR, which are known to be present in the perinuclear region as well as the nuclear compartment.[37-39] In contrast, other enzymes that might be targeted by **14** are known to localise to the ER/nuclear envelope network (PTP1B),[40] the cytosol and cytoskeletal

compartment (LMW-PTP),[41] or the cytosolic localisation (SHP-2).[39] While we cannot rule out the possibility that the observed localisation of **14** is influenced by other cysteine based phosphatases as well, it seems that in the cellular environment **14** is distributed throughout the cell in a pattern that matches the phosphatases it is targeting.

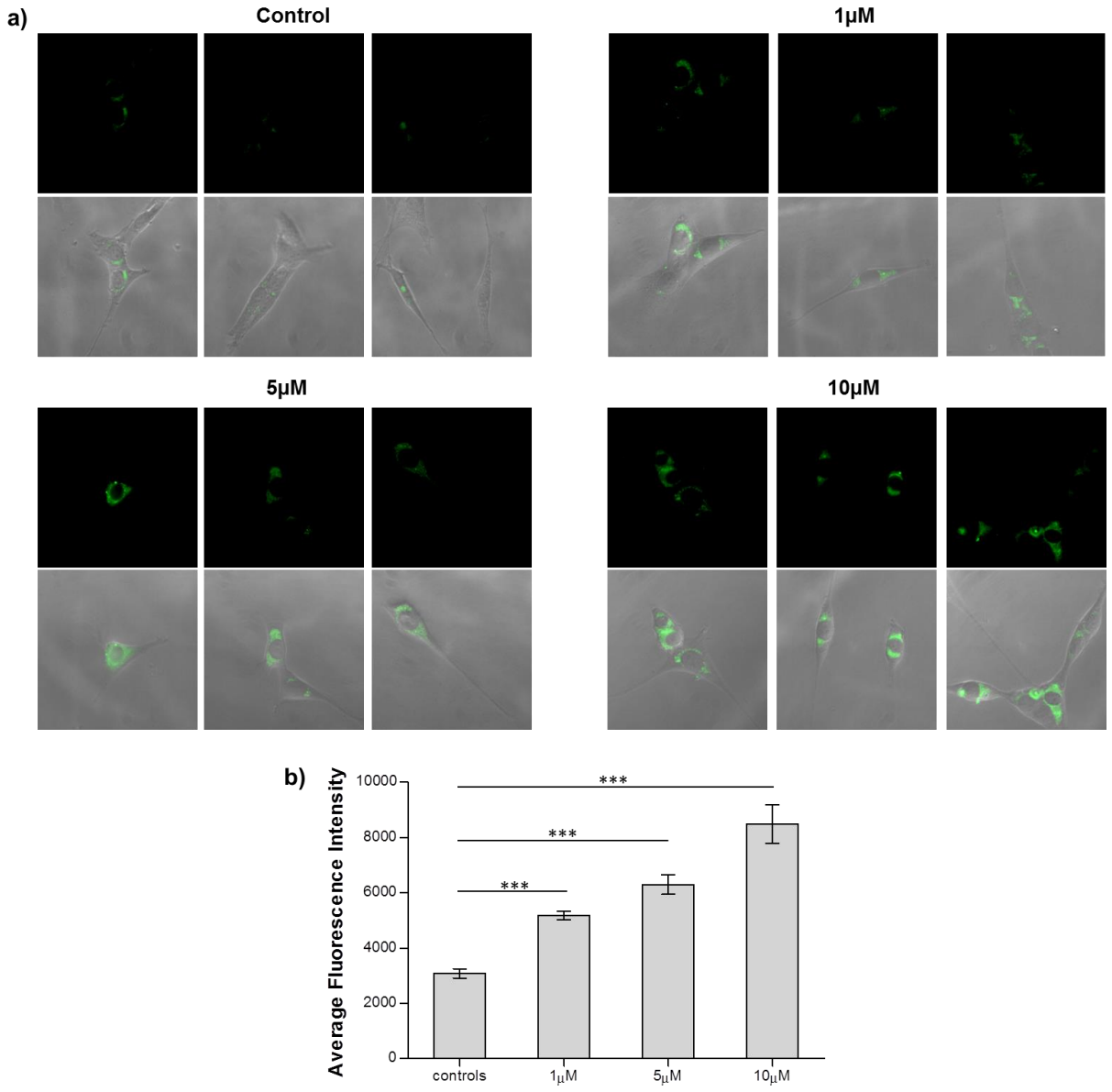

Fig. 6 (a) Fluorescence microscopy images showing uptake of **14** (green) by NIH3T3. Cells were incubated in media containing 0 μM (control), 1 μM, 5 μM or 10 μM of complex **14** and lastly fixed with PFA before imaging. To provide a better perception of the nuclear and perinuclear localisation of compound **14** three representative images are presented for each treatment in comparison with merge channel images. (b) Quantification of fluorescence signal was performed with FIJI. Data for the quantification are reported as ± SEM and were obtained from a minimum of 3 independent experiments counting a total number of cells as follow: 10 (for control), 7 (for 1 μM), 10 (for 5 μM),

18 (for 10 μM). Significant differences (5% cut-off for significance) to the control data are indicated by stars (*** $p < 0.001$).

Conclusions

Two new di-picolinic acid-based compounds containing a dansyl fluorophore have been prepared and successfully used as ligands to prepare the two novel vanadyl complexes **14** and **15**. Phosphatase inhibition assays showed that the complexes inhibited a selection of phosphatases (PTP1B, SHP-2, LMW-PTP, VHR and PTEN) over a concentration range of 72–222 nM and some selectivity and effect of linker length was observed. The variability in inhibition properties, together with fluorescence data for the complexes in the presence and absence of EDTA and enzyme indicate that the complexes are not simply acting as vanadyl delivery vehicles. On the other hand, based on their large size and saturated coordination sphere, it is unlikely that the intact complexes are binding to the enzymes and causing the inhibition of their activity. Therefore, we propose that derivatives of complexes **14** and **15** in which the ligand (**8** and **13** respectively) is partially de-coordinated from the vanadyl centre are interacting with the enzymes. A likely possibility could be that one of the picolinate 'arms' of the ligands de-coordinates leaving the vanadyl coordinatevely unsaturated and hence able to interact strongly with the enzymes and yet retain the fluorescent ligand (see Figure 7) as supported by the fluorescence studies. It has also been shown that the complexes are cell permeable and localize in the cytoplasm. The complexes represent a new class of tetradentate vanadyl inhibitors that offer the potential for synthetic functionalization. The data indicates that these new optically labelled vanadyl complexes have the potential to be developed further into potent and potentially selective inhibitors and targeted probes.

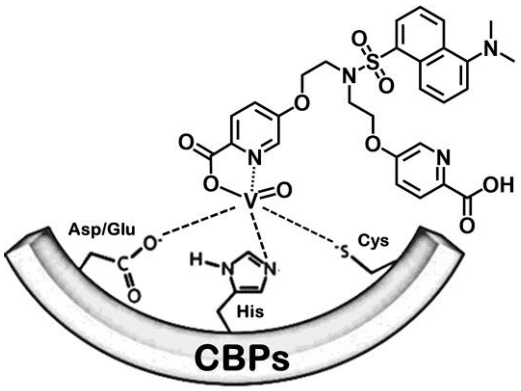

Fig. 7 Schematic representation of a potential binding mode between the vanadyl complexes and CBPs. This proposed interaction – based on the de-coordination of one 'arm' of the ligand – is consistent with the experimental observations herein presented.

Acknowledgements

This work was supported by Proxomics EPSRC Cross-Disciplinary Research Landscape Award (EP/I017887/1). L.H.M. is grateful for financial support from the Lowe Syndrome Trust UK. Dr David Gaboriau is acknowledged for his help with cell microscopy experiments performed at "The Facility for Imaging by Light Microscopy" (FILM, Imperial College London), supported by funding from the Wellcome Trust (grant P49828) and BBSRC (grant P48528)".

Experimental Details

General spectroscopy and materials. IR spectra were recorded on a Perkin Elmer FT–IR1720 Research Series spectrometer in the range 4000-600 cm^{-1}. Electrospray (ESI+) mass spectrometry was run at on a Waters Aquity UPLC I-CLASS coupled with Waters LCT Premier (operating in ES+ or ES- mode). MALDI analyses were performed using MicroMass MALDI microMX TOF operating in reflectron mode using a 337nm nitrogen laser. NMR

spectra were recorded on a Bruker spectrometer with d^6-DMSO (δ_H = 2.50 ppm, δ_C = 39.5 ppm), CD_3OD (δ_H = 3.31 ppm, δ_C = 49.2 ppm) and $CDCl_3$ (δ_H = 7.26 ppm, δ_C = 77.2 ppm) as internal references. UV-vis spectra were recorded on a Perkin-Elmer Lambda 25 UV-vis spectrometer. Fluorescence data were collected using a Varian fluorescence spectrometer, while fluorescence polarisation studies were performed with a Perkin-Elmer LS50B Luminescence Spectrometer. Compounds **3**, **4**, and **9** were prepared according to reported procedures.[34,42,43]

Synthesis of 5. To a solution of 5-hydroxyoxypicolinic acid methyl ester **3** (312 mg, 2.03 mmol), triphenylphosphine (1.07 g, 4.07 mmol) and *N*-Boc diethanolamine **4** (209 mg, 1.02 mmol) in anhydrous THF (15 mL), stirred on ice under N_2, was added diethyl azodicarboxylate (DEAD, 0.64 mL, 4.07 mmol) in anhydrous THF (1 mL). The resulting reaction mixture was stirred at room temperature for 16 hours. The solvent was removed by rotary evaporation to give the crude product **5** as an orange oil. The product was purified by silica gel column chromatography (70% EtOAc/Hex – 3% MeOH/EtOAc) to yield a mixture (ca. 1:0.1) of **5** and triphenylphosphine oxide. This compound was used without further purification for the next step. The following spectroscopic data corresponds to the signals associated to **5**: ^{1}H NMR (400 MHz, $CDCl_3$): δ(ppm) 8.37 (d, J = 2.9 Hz, 2H), 8.10 (d, J = 8.7 Hz, 2H), 7.26 (m, 2H), 4.24 (m, 4H), 3.98 (s, 1H,), 3.77 (t, J = 5.4 Hz, 4H), 1.46 (s, 9H). ^{13}C NMR (100 MHz, $CDCl_3$): δ(ppm) 165.2 (**C**), 157.4(**C**), 155.3 (**C**), 138.5 (**C**H), 138.3 (**C**H), 127.0 (**C**), 120.4 (**C**H), 67.4 (**C**H_2), 52.9 (**C**H_3), 48.2 (**C**H_2), 28.6 (**C**H_3). ESI-MS (+) 476 ($[M+H]^+$) (100%).

Synthesis of 6. To a solution of **5** (477 mg, 0.87 mmol) in dichloromethane (1 mL) was added trifluoroacetic acid (1 mL) and the reaction stirred at room temperature for 1 hour. The solvent was removed under reduced pressure and the product purified by silica gel column

chromatography (EtOAc then MeOH:dichloromethane: NEt_3 10:85:5) to give **6** (326 mg, 0.87 mmol, 100%) as a pale pink solid. ^{1}H NMR (400 MHz, $CDCl_3$): δ(ppm) 8.33 (d, J = 2.8 Hz, 2H), 8.09 (d, J = 8.7 Hz, 2H), 7.52 (dd, J = 8.8, 2.9 Hz, 2H), 4.35 (t, J = 5.0 Hz, 4H), 3.91 (s, 6H), 3.36 (t, J = 5.0 Hz). ^{13}C NMR (100 MHz, CD_3OD): δ(ppm) 166.2 (**C**), 159.0 (**C**), 141.2 (**C**H), 139.5 (**C**H), 127.9 (**C**), 122.2 (**C**H), 67.5 (**C**H_2), 53.0 (**C**H_3), 47.9 (**C**H_2). IR in cm^{-1} υ(C-H)/υ(N-H) 3059-2955, υ(C=N)/υ(C=C) 1735, 1668,1623, 1578, υ(C-O) 1303. LC-MS(+) 377 ($[M+H]^+$) (100%).

Synthesis of 7. To a solution of **6** (100 mg, 0.27 mmol) and dansyl chloride (87 mg, 0.32 mmol) in anhydrous acetonitrile (8.5 mL) was added anhydrous triethylamine (0.08 mL, 0.54 mmol) and the reaction stirred at room temperature for 16 h. The solvent was removed by rotary evaporation to give a yellow residue. The crude mixture was purified by silica gel column chromatography (2% MeOH in dichloromethane) to give the desired product **7** (83 mg, 0.14 mmol, 50%) as a yellow/green oil. ^{1}H NMR (400 MHz, CD_3OD): δ(ppm) 8.50 (dt, J = 8.6, 1.0 Hz, 1H), 8.24 (dd, J = 7.3, 1.2 Hz, 1H), 8.21-8.18 (m, 1H), 8.01-7.90 (m, 4H), 7.52 (dd, J = 8.5, 7.3 Hz, 1H) 7.41 (dd, J = 8.7, 7.6 Hz, 1H), 7.19 (dd, J = 8.8, 2.9 Hz, 2H), 7.13 (dd, J = 7.7, 0.8 Hz, 1H), 4.21 (t, J = 5.2 Hz, 4H), 3.91 (m, 10H), 2.81 (s, 6H). ^{13}C NMR (100 MHz, CD_3OD): δ(ppm) 166.2 (**C**), 158.8 (**C**), 153.2 (**C**), 140.8 (**C**H), 139.3 (**C**H), 136.1 (**C**), 131.9 (**C**), 131.3, 131.2 (**C**H), 131.1 (**C**H), 129.2 (**C**H), 127.7 (**C**), 124.3 (**C**H), 121.8 (**C**H), 120.5 (**C**), 116.4 (**C**H), 68.2 (**C**H_2), 53.0 (**C**H_3), 45.7 (**C**H_2). ESI-MS (+) 609 ($[M+H]^+$). IR in cm^{-1} υ(C=N)/υ(C=C) 1715, 1573.

Synthesis of 8. To a solution of **7** (196 mg, 0.32 mmol) in THF:MeOH (0.8:0.3 mL) on ice was added 6M NaOH (0.15 mL, 0.90 mmol) and the reaction stirred for 3 hours at room temperature. The solvent was removed by rotary evaporation to give a bright yellow solid which was diluted with water and extracted with ethyl acetate. The organic layer was set

aside and the aqueous layer acidified with 2M HCl and re-extracted with EtOAc (4 x 10 mL). The organic layers were combined, dried over Mg_2SO_4 and the solvent removed by rotary evaporation to give the desired product **8** (98.5 mg, 0.17 mmol, 53%) as a yellow solid. ^{1}H NMR (400 MHz, CD_3OD): δ(ppm) 8.51 (d, J = 8.6 Hz, 1H), 8.25 (d, J = 7.4, 1.2 Hz, 1H), 8.20 (d, J = 8.7 Hz, 1H), 8.06-7.92 (m, 4H), 7.53 (dd, J = 8.5, 7.3 Hz, 1H), 7.42 (dd, J = 8.7, 7.6 Hz, 1H), 7.21 (dd, J = 8.7, 2.9 Hz, 2H), 7.13 (d, J = 7.5 Hz, 1H), 4.21 (t, J = 5.2 Hz, 4H), 3.93 (t, J = 5.2 Hz, 4H), 2.83 (s, 6H). ^{13}C NMR (100 MHz, DMSO-d^6): δ(ppm) 165.7 (**C**), 156.5 (**C**), 151.4 (**C**), 140.6 (**C**H), 137.7 (**C**H), 134.8 (**C**), 130.1 (**C**), 129.4, 129.2 (**C**H), 128.9 (**C**H), 128.1 (**C**H), 126.1 (**C**), 123.6 (**C**H), 120.6 (**C**H), 118.8 (**C**), 115.2 (**C**H), 66.4 (**C**H_2), 46.8 (CH_3), 45.0 (**C**H_2). ESI-MS (+) 581 ($[M+H]^+$). IR in cm^{-1} υ(C=N)/υ(C=C) 1690, 1573, υ(S=O) 1140. Fluorescence in DMF: λ_{max}(ex) 358 nm, λ_{max}(em) 538 nm.

Synthesis of 14. To a suspension of **8** (167 mg, 0.29 mmol) in water (6 mL) was added 10% $NaHCO_3$ (0.51 mL, 0.58 mmol) and the mixture stirred until all solid was dissolved. $VOSO_4$ (63 mg, 0.29 mmol) in water (4 mL) was added slowly over 2 minutes after which a precipitate began to form. The reaction was left to stir for 2 hours. After 1 week without stirring a green solid precipitated from the solution. This was collected by filtration and IR indicated a vanadyl complex had formed. Further characterisation by mass spectrometry indicated this was the desired complex **14** (13 mg, 0.02 mmol, 7%). ESI-MS (+) 668 ($[M+Na]^+$). IR in cm^{-1} υ(C=N)/υ(C=C) 1636, 1591, 1575, υ(S=O) 1136, υ(V=O) 965. Calc. for $C_{28}H_{26}O_9N_4SV\cdot 3H_2O$: C 48.07, H 4.61, N 8.01 Found: C 48.07, H 4.39, N 7.72. UV-vis (MeOH/DMF) λ/nm (ε/$M^{-1}\cdot cm^{-1}$) 263 (4.86×10^4), 337 (1.03×10^4). Fluorescence in Tris buffer: λ_{max}(ex) 340 nm, λ_{max}(em) 568 nm.

Synthesis of 10. To a solution of 5-hydroxypicolinic acid methyl ester **3** (362 mg, 2.36 mmol), triphenylphosphine (1.24 g, 4.72 mmol) and *N*-Boc dipropanolamine **9** (276 mg, 1.18

mmol) in anhydrous THF (18 mL), stirred on ice under N_2, was added diethyl azodicarboxylate (DEAD, 0.74 mL, 4.72 mmol) in anhydrous THF (1.2 mL) and the reaction was stirred at room temperature for 16 h. Solvent was removed by rotary evaporation to give the crude product **10** as an orange oil. The product was purified by silica gel column chromatography (80% EtOAc/Hex – 3% MeOH/EtOAc) to yield a mixture (*ca*. 1:0.2) of **10** and triphenylphosphine oxide. This compound was used without further purification for the next step. The following spectroscopic data corresponds to the signals associated to **10**: ^{1}H NMR (400 MHz, $CDCl_3$): δ(ppm) 8.37 (d, J = 2.9 Hz, 2H), 8.10 (d, J = 8.7 Hz, 2H), 7.24 (dd, J = 8.8, 2.9 Hz, 2H), 4.13-4.08 (m, 4H), 3.97 (s, 6H), 3.41 (t, J = 6.9 Hz, 4H), 2.16-2.03 (m, 4H), 1.39 (s, 9H).

Synthesis of 11. To a solution of **10** (421 mg, 0.95 mmol) in dichloromethane (1 mL) was added trifluoroacetic acid (1 mL) and the reaction stirred at room temperature for 1 hour. The solvent was removed and the product **11** isolated pure by silica gel column chromatography (EtOAc then MeOH:dichloromethane:NEt_3 10:85:5) to give the desired product **11** (279 mg, 0.67 mmol, 71%) as a pale pink solid. ^{1}H NMR (400 MHz, d6-DMSO): δ(ppm) 8.37 (d, J = 2.8 Hz, 2H), 8.03 (d, J = 8.7 Hz, 2H), 7.50 (dd, J = 8.8, 2.9 Hz, 2H), 4.21 (t, J = 6.2 Hz, 4H), 3.84 (s, 6H), 2.91 (t, J = 7.1 Hz, 4H), 2.00 (m, 4H). ^{13}C NMR (100 MHz, d6-DMSO): δ(ppm) 164.8 (**C**), 157.2 (**C**), 139.5 (**C**H), 139.4 (**C**H), 126.4 (**C**), 120.6 (**C**H), 66.1 (**C**H_2), 52.1 (**C**H_3), 44.9 (**C**H_2), 27.1 (**C**H_2). IR in cm^{-1} υ(N-H) 2804, υ(C=N)/υ(C=C) 1732, 1669, 1574, υ(C-O) 1316. ESI-MS (+) 404 ($[M+H]^+$), 426 ($[M+Na]^+$).

Synthesis of 12. To a solution of **11** (270 mg, 0.67 mmol) and dansyl chloride (217 mg, 0.80 mmol) in anhydrous acetonitrile (21 mL) was added anhydrous triethylamine (0.28 mL, 2.0 mmol) and the reaction stirred at room temperature for 48 h. The solvent was removed by rotary evaporation to give a yellow residue. The crude mixture was purified by silica gel

column chromatography (2- 3% MeOH in dichloromethane) to give the desired product **12** (317 mg, 0.50 mmol, 75%) as a yellow solid.. ^{1}H NMR (400 MHz, CD_3OD): δ(ppm) 8.26 (dt, J = 8.6, 1.0 Hz, 1H), 8.21 (dd, J = 7.4, 1.2 Hz, 1H), 8.13 (d, J = 8.7, 0.9 Hz, 1H), 8.04 (d, J = 2.9 Hz, 2H), 7.99 (d, J = 8.8 Hz, 2H), 7.54-7.46 (m, 2H), 7.12 (dd, J = 8.7, 2.9 Hz, 2H), 7.09 (d, J = 7.7, 0.8 Hz, 1H), 3.96-3.93 (m, 10H), 3.59 (t, 4H, J = 6.7 Hz), 2.77 (s, 6H) 2.08 (m, 4H). ^{13}C NMR (100 MHz, CD_3OD): δ(ppm) 166.3 (**C**), 159.1 (**C**), 153.1 (**C**), 140.5 (**C**H), 139.3 (**C**H), 135.3 (**C**), 131.9 (**C**), 131.7, 131.2 (**C**H), 130.9 (**C**H), 129.2 (**C**H), 127.7 (**C**), 124.1 (**C**H), 121.6 (**C**H), 120.0 (**C**), 116.0 (**C**H), 66.7 (**C**H_2), 53.0 (**C**H_3), 45.7 (**C**H_2), 43.6 (**C**H_2), 28.0 (**C**H_2). ESI-MS (+) 637 ($[M+H]^+$), 659 ($[M+Na]^+$).

Synthesis of 13. To a solution of **12** (317 mg, 0.50 mmol) in THF:MeOH (1.3:0.5 mL) on ice was added 6M NaOH (0.23 mL, 1.90 mmol) and the reaction stirred for 3 h at room temperature. The solvent was removed by rotary evaporation to give a pale yellow solid which was diluted with water and extracted with ethyl acetate. The organic layer was set aside and the aqueous layer acidified with 6M HCl and re-extracted with EtOAc (3×6 mL) and dichloromethane (1 × 6 mL). The organic layers were combined, dried over Mg_2SO_4 and the solvent removed by rotary evaporation to give the desired product **13** (157 mg, 0.26 mmol, 52%) as a yellow solid. ^{1}H NMR (400 MHz, CD_3OD): δ(ppm) 8.27 (d, J = 8.5 Hz, 1H), 8.22 (d, J = 7.4 Hz, 1H), 8.14 (d, J = 8.4 Hz, 1H), 8.06 (d, J = 2.8 Hz, 2H), 8.02 (d, J = 8.8 Hz, 2H), 7.54-7.48 (m, 2H), 7.17 (dd, J = 8.7, 2.9 Hz, 2H), 7.12 (d, J = 7.6 Hz, 1H), 3.96 (t, J = 5.8 Hz, 4H), 3.60 (t, 4H, J = 6.8), 2.79 (s, 6H), 2.12 – 2.05 (m, 4H). ^{13}C NMR (100 MHz, d^6-DMSO): δ(ppm) 165.7 (**C**), 156.8 (**C**), 151.4 (**C**), 140.3 (**C**H), 137.7 (**C**H), 134.2 (**C**), 130.1 (**C**), 129.4, 129.3 (**C**H), 129.1 (**C**H), 128.1 (**C**H), 126.1 (**C**), 123.5 (**C**H), 120.4 (**C**H), 118.5 (**C**), 115.0 (**C**H), 65.4 (**C**H_2), 45.0 (**C**H_2), 43.1 (**C**H_2), 27.0 (**C**H_2). ESI-MS (+) 609 ($[M+H]^+$). Fluorescence in DMF: λ_{max}(ex) 340 nm, λ_{max}(em) 528 nm.

Synthesis of 15. To a suspension of **13** (150 mg, 0.25 mmol) in water (6 mL) was added 10% $NaHCO_3$ (0.44 mL, 0.49 mmol) and the mixture stirred until all solid was dissolved. A solution of $VOSO_4$ (53.5 mg, 0.25 mmol) in water (3.5 mL) was added slowly over 2 minutes after which a precipitate began to form. The reaction was left to stir for 2 hours. After 2 days without stirring a green solid had precipitated from the reaction solution which was collected by filtration and IR indicated a vanadyl complex had formed. Further characterisation by mass spectrometry indicated this was the desired complex **15** (42 mg, 0.06 mmol, 25%). ESI-MS (+) 696 ($[M+Na]^+$). IR in cm^{-1} υ(C=N)/υ(C=C) 1645,1591, 1572, υ(S=O) 1134, υ(V=O) 961. Calc. for $C_{30}H_{30}O_9N_4SV \cdot 3.5H_2O$: C 48.92, H 5.06, N 7.61 Found: C 48.62, H 4.71, N 7.39. UV-vis (MeOH/DMF) λ/nm (ε/$M^{-1} \cdot cm^{-1}$) 262 (7.37×10^4), 340 (1.30×10^4). Fluorescence in Tris buffer: λ_{max}(ex) 340 nm, λ_{max}(em) 566 nm.

CBP Expression and Purification. PTP1B, VHR, SHP2 and LMW-PTP were expressed as GST-fusion proteins. The protocol followed was: the corresponding RNA was extracted using PureLink® RNA Mini Kit from Invitrogen (according to manufacturer's protocol) from HEK293 cells. First DNA synthesis was performed using ProtoScript® First Strand cDNA Synthesis Kit from New England Biolabs according to manufacturer's protocol. In a second round of PCR, gene specific primers were used to obtain the DNA for PTEN, PTP1B, VHR, SHP2 and LMW-PTP, adding the restriction site BamHI at 5' and XhoI at the 3' end, respectively. The obtained DNA fragments were then cloned into pGEX-6P-1 vector using the aforementioned restriction sites. All four constructs were validated via DNA sequencing to ensure in-frame cloning with the GST tag encoded by the pGEX-6P-1 vector.

Protein expression was induced in the *E. coli* strain DH5α for 24h using 1 mM IPTG at 23° C. After growth the cells were harvested and stored at -20°C. The harvested cells were

resuspended in lysis buffer containing 50 mM Tris (pH 7.4), 1% Triton X-100, 10 mM benzamidine hydrochloride, 100 µg/mL soybean trypsin inhibitor, 1 mM 4-(2-Aminoethyl)benzenesulfonyl fluoride hydrochloride and 2 mM DTT. Lysozyme was added to the cell suspension at a concentration of 2 mg/mL and stirred for 1 h at 4°C. Lysis was completed by sonication, followed by centrifugation at 18000 g for 30 min at 4°C. The supernatant was loaded onto a glutathione sepharose column, pre-equilibrated with 50 mM Tris (pH 7.4), 140 mM NaCl and 2.7 mM KCl. After loading, the column was washed twice with 50 mM Tris (pH 7.4), 140 mM NaCl, 2.7 mM KCl and 2 mM DTT. Another two washes were performed using the same buffer with 500 mM NaCl. The GST-tagged phosphatases were eluted using 20 mM glutathione in 50 mM Tris (pH 7.4), 250 mM NaCl and 2 mM DTT. 50 % glycerol was added and the proteins were stored at -80°C. Protein concentration was determined using Bradford assay.

Phosphatase inhibition assays in the absence of EDTA. 3-*O*-methylfluorescein phosphate (OMFP, 10 mM in DMSO) was diluted with a 1% DMSO solution to the required concentration. The corresponding vanadyl complexes were dissolved in DMF or DMSO to 10 mM and further diluted in water containing 1% DMSO to the required concentrations. Assays were run in 100 mM Tris (pH7.4) containing 1 mM DTT at room temperature. The inhibitor solutions were incubated with the enzyme in the buffer for 10 minutes at room temperature before reaction was initiated by addition of OMFP. Hydrolysis of OMFP to OMF was monitored by measuring changes in fluorescence over 30 minutes at 60 s intervals (excitation 485 nm, emission 525 nm) using a Varian fluorescence spectrometer. Enzyme free blanks were run to eliminate background effects of OMFP hydrolysis in solution.

Statistical analysis of enzyme inhibition data. Statistical comparison of the means (using GraphPad Prism 5 or StatPlus, AnalystSoft Inc.) was performed by a two-tailed t-test. A 5%

cut-off for significance was employed and the degree of significance indicated by stars (i.e. * $p < 0.05$; ** $p < 0.01$; *** $p < 0.001$) within the corresponding figures.

Changes in fluorescence of complexes in presence of enzyme and/or EDTA. Vanadyl compounds were dissolved in DMF to 10 mM and further diluted in buffer containing 1% DMSO to 300 µM. Enzyme was added to buffer solution of 100 mM Tris (pH7.4) containing 1 mM DTT, with or without 1 mM EDTA. Enzyme free controls consisted of buffer solution of 100 mM Tris (pH=7.4) containing 1 mM DTT, with or without 1 mM EDTA. In a 96-well plate, the inhibitor solutions were added to wells containing one of the above mentioned buffers to a final concentration of 30 µM. Fluorescence emission spectra were recorded in the range of 380-650 nm after excitation at 340 nm with excitation slit widths of 5-10 nm and emission slit widths of 10-20 nm using a Varian fluorescence spectrometer. Readings were taken 5 minutes and 2 hours after addition of inhibitor solutions.

Fluorescence Anisotropy Measurements: Vanadium complexes were dissolved in DMSO to 10 mM and further diluted in a 1% DMSO solution to the required concentration. A five-fold excess of enzyme was diluted in an aqueous solution of 1 mM DTT and 100 mM Tris (pH 7.4) and incubated with the inhibitor for 10 mins. A 50:50 glycerol-elution buffer (100mM Tris, 250 mM NaCl, 20 mM reduced glutathione, 2 mM DTT, pH 7.4) mixture was used for the enzyme free control. Samples were then analysed for polarised fluorescence emission in a fluorescence cuvette (excitation 340 nm, emission 560 nM). 1mM EDTA was then added to the enzyme containing solution and further readings were taken every 15 mins for 60 mins and then a final reading at 100 mins.

Fluorescence Anisotropy Measurements – enzyme titration: Vanadium complexes were dissolved in DMSO to 10 mM and further diluted in a 1% DMSO solution to the required concentration before mixing with an aqueous solution of 1 mM DTT and 100 mM Tris (pH 7.4). A fluorescence anisotropy reading was taken at excitation 340 nM, emission 560 nM. LMW-PTP was then titrated into the mixture increasing from 0.36 equivalent to 3.6 equivalents with a fluorescence anisotropy reading taken after 1 min incubation with each enzyme addition.

Cell uptake studies. NIH3T3 cells were grown in Dulbecco's modified Eagle's medium (DMEM) supplemented with 10% newborn calf serum in an atmosphere of 10 % CO_2 at 37ºC. Cells were seeded in a plastic 24-well plate. After 16 hours the compound was added to the cells in fresh media at 1, 5 and 10 μM (final DMSO concentration 1 % v/v for all wells), and incubated for 24 hours at 37ºC and 10% CO_2. The media was then removed and the cells washed three times with sterile Dulbecco's phosphate buffered saline (PBS, EDTA-free). The cells were fixed by adding 4% paraformaldehyde (PFA) for 15 minutes at room temperature. The coverslips were then washed a further three times with PBS and. processed to fluorescence microscopy experiments using a Zeiss Axiovert 200 inverted microscope with filter for FITC (excitation wavelength 465 – 495 nm, emission wavelength 515 – 555 nm). Images were acquired using a Hammamatsu Flash 4 (2048x2048 pixel) camera for each channel separately and processed using Volocity Software.

References and Notes

1. A. Salmeen and D. Barford, *Antioxid. Redox Signaling*, 2005, **7**, 560-577.

2. B. Vanhaesebroeck, S. J. Leevers, K. Ahmadi, J. Timms, R. Katso, P. C. Driscoll, R. Woscholski, P. J. Parker and M. D. Waterfield, *Annu. Rev. Biochem.*, 2001, **70**, 535-602.

3. K. Kolmodin and J. Aqvist, *FEBS Lett.*, 2001, **498**, 208-213.

4. A. Ostman, C. Hellberg and F. D. Bohmer, *Nature Reviews Cancer*, 2006, **6**, 307-320.

5. J. L. Low, C. L. Chai and S. Q. Yao, *Antioxid. Redox Signal*, 2014, **20**, 2225-2250.

6. J. M. Dyson, C. G. Fedele, E. M. Davies, J. Becanovic and C. A. Mitchell, *Subcell. Biochem.*, 2012, **58**, 215-279.

7. C. Yuan, L. Lu, Y. Wu, Z. Liu, M. Guo, S. Xing, X. Fu and M. Zhu, *J. Inorg. Biochem.*, 2010, **104**, 978-986.

8. Q. Wang, M. Zhu, L. Lu, C. Yuan, S. Xing and X. Fu, *Dalton Trans.*, 2011, **40**, 12926-12934.

9. R. He, L. F. Zeng, Y. He, S. Zhang and Z. Y. Zhang, *FEBS Journal*, 2013, **280**, 731-750.

10. L. Lu, S. Wang, M. Zhu, Z. Liu, M. Guo, S. Xing and X. Fu, *Biometals*, 2010, **23**, 1139-1147.

11. L. P. Lu and M. L. Zhu, *Anti-Cancer Agents Med. Chem.*, 2011, **11**, 164-171.

12. A. C. Schmid and R. Woscholski, *Biochem. Soc. Trans.*, 2004, **32**, 348-349.

13. L. M. Scott, H. R. Lawrence, S. M. Sebti, N. J. Lawrence and J. Wu, *Curr. Pharm. Des.*, 2010, **16**, 1843-1862.

14. Z. Y. Zhang, *Annu. Rev. Pharmacol. Toxicol.*, 2002, **42**, 209-234.

15. L. P. Lu and M. L. Zhu, *Antioxid. Redox Signal*, 2014, **20**, 2210-2224.

16. M. Nakai, F. Sekiguchi, M. Obata, C. Ohtsuki, Y. Adachi, H. Sakurai, C. Orvig, D. Rehder and S. Yano, *J. Inorg. Biochem.*, 2005, **99**, 1275-1282.

17. K. H. Thompson and C. Orvig, *J. Inorg. Biochem.*, 2006, **100**, 1925-1935.

18. C. C. McLauchlan, B. J. Peters, G. R. Willsky and D. C. Crans, *Coord. Chem. Rev.*, 2015, **301-302**, 163-199.

19. J. Costa Pessoa, E. Garribba, M. F. A. Santos and T. Santos-Silva, *Coord. Chem. Rev.*, 2015, **301-302**, 49-86.

20. C. Cuncic, S. Desmarais, N. Detich, A. S. Tracey, M. J. Gresser and C. Ramachandran, *Biochem. Pharmacol.*, 1999, **58**, 1859-1867.

21. B. I. Posner, R. Faure, J. W. Burgess, A. P. Bevan, D. Lachance, G. Y. Zhangsun, I. G. Fantus, J. B. Ng, D. A. Hall, B. S. Lum and A. Shaver, *J. Biol. Chem.*, 1994, **269**, 4596-4604.

22. M. W. Makinen and M. Salehitazangi, *Coord. Chem. Rev.*, 2014, **279**, 1-22.

23. G. Huyer, S. Liu, J. Kelly, J. Moffat, P. Payette, B. Kennedy, G. Tsaprailis, M. J. Gresser and C. Ramachandran, *J. Biol. Chem.*, 1997, **272**, 843-851.

24. C. C. McLauchlan, J. D. Hooker, M. A. Jones, Z. Dymon, E. A. Backhus, B. A. Greiner, N. A. Dorner, M. A. Youkhana and L. M. Manus, *J. Inorg. Biochem.*, 2010, **104**, 274-281.

25. M. Li, W. Ding, B. Baruah, D. C. Crans and R. Wang, *J. Inorg. Biochem.*, 2008, **102**, 1846-1853.

26. B. I. Posner, R. Faure, J. W. Burgess, A. P. Bevan, D. Lachance, G. Zhang-Sun, I. G. Fantus, J. B. Ng, D. A. Hall and et al., *J. Biol. Chem.*, 1994, **269**, 4596-4604.

27. D. C. Crans, A. D. Keramidas, H. Hoover-Litty, O. P. Anderson, M. M. Miller, L. M. Lemoine, S. Pleasic-Williams, M. Vandenberg, A. J. Rossomando and L. J. Sweet, *J. Am. Chem. Soc.*, 1997, **119**, 5447-5448.

28. L. H. Mak, R. Vilar and R. Woscholski, *J. Chem. Biol.*, 2010, **3**, 157-163.

29. E. Rosivatz, J. G. Matthews, N. Q. McDonald, X. Mulet, K. K. Ho, N. Lossi, A. C. Schmid, M. Mirabelli, K. M. Pomeranz, C. Erneux, E. W. F. Lam, R. Vilar and R. Woscholski, *ACS Chem. Biol.*, 2006, **1**, 780-790.

30. A. C. Schmid, R. D. Byrne, R. Vilar and R. Woscholski, *FEBS Lett.*, 2004, **566**, 35-38.

31. A. P. Seale, L. A. de Jesus, S. Y. Kim, Y. H. Choi, H. B. Lim, C. S. Hwang and Y. S. Kim, *Biotechnol. Lett.*, 2005, **27**, 221-225.

32. E. Lodyga-Chruscinska, G. Micera and E. Garribba, *Inorg. Chem.*, 2011, **50**, 883-899.

33. H. Sakurai, K. Fujii, H. Watanabe and H. Tamura, *Biochem. Biophys. Res. Commun.*, 1995, **214**, 1095-1101.

34. G. Mercey, T. Verdelet, G. Saint-Andre, E. Gillon, A. Wagner, R. Baati, L. Jean, F. Nachon and P. Y. Renard, *Chem. Comm.*, 2011, **47**, 5295-5297.

35. J. C. Pessoa, I. Cavaco, I. Correia, I. Tomaz, P. Adao, I. Vale, V. Ribeiro, M. M. C. A. Castro and C. C. F. G. Geraldes, *ACS Symp. Ser.*, 2007, **974**, 340-351.

36. A. Levina, A. I. McLeod, A. Pulte, J. B. Aitken and P. A. Lay, *Inorg. Chem.*, 2015, **54**, 6707-6718.

37. J. Zhang, P. Zhang, Y. Wei, H.-l. Piao, W. Wang, S. Maddika, M. Wang, D. Chen, Y. Sun, M.-C. Hung, J. Chen and L. Ma, *Nat. Cell Biol.*, 2013, **15**, 1486-1494.

38. S. M. Walker, C. P. Downes and N. R. Leslie, *Biochem. J.*, 2001, **360**, 277-283.

39. R. Xu, Y. Yu, S. Zheng, X. Zhao, Q. Dong, Z. He, Y. Liang, Q. Lu, Y. Fang, X. Gan, X. Xu, S. Zhang, Q. Dong, X. Zhang and G.-S. Feng, *Blood*, 2005, **106**, 3142-3149.

40. I. Anderie, I. Schulz and A. Schmid, *Cell. Signalling*, 2007, **19**, 582-592.

41. P. Cirri, P. Chiarugi, L. Taddei, G. Raugei, G. Camici, G. Manao and G. Ramponi, *J. Biol. Chem.*, 1998, **273**, 32522-32527.

42. C. Granier and R. Guilard, *Tetrahedron*, 1995, **51**, 1197-1208.

43. Y. Uto, Y. Kiyotsuka, Y. Ueno, Y. Miyazawa, H. Kurata, T. Ogata, T. Deguchi, M. Yamada, N. Watanabe, M. Konishi, N. Kurikawa, T. Takagi, S. Wakimoto, K. Kono and J. Ohsumi, *Bioorg. Med. Chem. Lett.*, 2010, **20**, 746-754.